HHS Public Access

Author manuscript

Gastroenterology. Author manuscript; available in PMC 2016 April 01.

Published in final edited form as:

Gastroenterology. 2015 April ; 148(4): 771–782.e11. doi:10.1053/j.gastro.2014.12.034.

Mutations in *RAD21* Disrupt Regulation of APOB in Patients with Chronic Intestinal Pseudo-obstruction

Elena Bonora[1], **Francesca Bianco**[1], **Lina Cordeddu**[2], **Michael Bamshad**[3], **Ludmila Francescatto**[4], **Dustin Dowless**[4], **Vincenzo Stanghellini**[1], **Rosanna F. Cogliandro**[1], **Greger Lindberg**[2], **Zeynel Mungan**[5], **Kivanc Cefle**[6], **Tayfun Ozcelik**[7], **Sukru Palanduz**[6], **Sukru Ozturk**[6], **Asuman Gedikbasi**[6], **Alessandra Gori**[1], **Tommaso Pippucci**[1], **Claudio Graziano**[1], **Umberto Volta**[1], **Giacomo Caio**[1], **Giovanni Barbara**[1], **Mauro D'Amato**[2], **Marco Seri**[1], **Nicholas Katsanis**[4], **Giovanni Romeo**[1,*], and **Roberto De Giorgio**[1,8]

[1]Department of Medical and Surgical Sciences, University of Bologna, and St. Orsola-Malpighi Hospital, Bologna, Italy

[2]Karolinska Institutet, Stockholm, Sweden

[3]University of Washington Center for Mendelian Genomics, Seattle, USA

[4]Center for Human Disease Modeling Duke University, Durham, USA

[5]Koc University of Istanbul, Istanbul, Turkey

[6]Istanbul Medical Faculty, Dept. of Internal Medicine, Division of Medical Genetics

[7]Bilkent University, Bilkent, Ankara, Turkey

[8]Centro Unificato di Ricerca Biomedica Applicata (CRBA), Bologna, Italy

Abstract

Background & Aims—Chronic intestinal pseudo-obstruction (CIPO) is characterized by severe intestinal dysmotility that mimicks a mechanical sub-occlusion with no evidence of gut obstruction. We searched for genetic variants associated with CIPO to increase our understanding of its pathogenesis and indentify potential biomarkers.

Corresponding authors: Roberto De Giorgio, MD, PhD, AGAF, Department of Medical and Surgical Sciences, University of Bologna, St. Orsola-Malpighi Hospital, via Massarenti 9, 40138 Bologna, Italy, Tel: +390516363558; Fax: +39051345864; roberto.degiorgio@unibo.it and/or: Giovanni Romeo, MD, PhD, Department of Medical and Surgical Sciences, University of Bologna, St. Orsola-Malpighi Hospital, via Massarenti 9, 40138 Bologna, Italy. Tel:+390512088421; Fax: +390512088416; egf.giovanni.romeo@gmail.com.

Conflict of interest: The authors declare no conflict of interest

Author contributions: Study concept and design: EB, RDG, NK; acquisition of data: FB, LC, DD, LF, AG, RC, GL, CG; analysis and interpretation of data: EB, MDA, TP, MB, RDG; drafting of the manuscript: EB, RDG, NK, GR; critical revision of the manuscript for important intellectual content: MDA, NK, EB, RDG, GR, GL, MS, VS, MB; statistical analysis: EB, FB, DD, LF; obtained funding: RDG, NK, MB, GR; material support: GL, ZM, KC, TO, AG, SP, SO, UV, GC, GB; study supervision: RDG, EB, GR, NK.

Methods—We performed whole-exome sequencing of genomic DNA from patients with familial CIPO syndrome. Blood and lymphoblastoid cells were collected from patients and controls (individuals without CIPO); levels of mRNA and proteins were analyzed by quantitative reverse transcription PCR, immunoblot, and mobility shift assays. cDNAs were transfected into HEK293 cells. Expression of *rad21* was suppressed in zebrafish embryos using a splice-blocking morpholino (*rad21a* MO). Gut tissues were collected and analyzed.

Results—We identified a homozygous mutation (p.622, encodes Ala>Thr) in *RAD21* in patients from a consanguineous family with CIPO. Expression of *RUNX1*, a target of RAD21, was reduced in cells from patients with CIPO compared with controls. In zebrafish, suppression of *rad21a* reduced expression of *runx1*; this phenotype was corrected by injection of human *RAD21* mRNA, but not with the mRNA from the mutated p.622 allele. *rad21a MO* zebrafish had delayed intestinal transit and greatly reduced numbers of enteric neurons, similar to patients with CIPO. This defect was greater in zebrafish with suppressed expression of *ret* and *rad21*, indicating their interaction in regulation of gut neurogenesis. The promoter region of *APOB* bound RAD21 but not RAD21 p. 622 Ala>Thr; expression of wild-type RAD21 in HEK293 cells repressed expression of *APOB*, compared with control vector. The gut-specific isoform of APOB (APOB48) is overexpressed in sera from patients with CIPO who carry the RAD21 mutation. APOB48 is also overexpressed in sporadic CIPO in sera and gut biopsies.

Conclusions—Some patients with CIPO carry mutations in *RAD21* that disrupt the ability of its product to regulate genes such as *RUNX1* and *APOB*. Reduced expression of *rad21* in zebrafish, and dysregulation of these target genes, disrupts intestinal transit and development of enteric neurons.

Keywords

sporadic and familial chronic intestinal pseudo-obstruction; intestinal motility; animal model; genetic analysis

Introduction

Chronic intestinal pseudo-obstruction (CIPO), a rare and potentially life-threatening disorder with unknown prevalence and incidence,[1–3] is viewed typically as an insufficiency of the intestinal peristalsis that mimicks a sub-occlusive disease in the absence of mechanical obstructions.[4–6] The severity of the clinical presentation and the limited understanding of the disorder contribute to poor quality of life and increased mortality.[2,4–7] In addition, there are no specific biochemical or molecular biomarkers of CIPO, hindering further a correct diagnosis. From a genetic perspective, most CIPO patients are sporadic, although X-linked, autosomal dominant and recessive forms have been identified with mutations in filamin A (*FLNA*)[8,9], actin G2 (*ACTG2*)[10], thymidine phosphorylase (*TYMP*)[11] / polymerase gamma (*POLG1*)[12] and more recently in *SGOL1*.[13] However, the underlying genetic alterations and molecular mechanisms remain unknown in most CIPO cases.

We previously mapped a locus in a large consanguineous family segregating an autosomal recessive form of CIPO.[14,15]In the affected family members, the major clinical feature was represented by CIPO, in addition to megaduodenum, long-segment Barrett esophagus, and

cardiac abnormalities of variable severity (OMIM 611376; Mungan syndrome, MGS). Here, we intersected mapping data with WES to identify *RAD21* as a causal locus for CIPO. Our combined genetic and functional data suggest a loss of function mechanism that disrupts the structure and function of enteric innervation. Moreover, based on our previous observations that identified Apolipoprotein B (APOB) as a target of RET signaling,[16] we explored the role of this protein in CIPO etiopathology in the context of RAD21 mutations. Here we report a key role for APOB48, a gut-specific isoform[17] as a transcriptional target of RAD21, and thus a contributor to CIPO, with a potential utility as a biomarker.

Methods

Patients and controls

The clinical characteristics of the patients with syndromic CIPO are indicated in the Supplementary Material. An additional 21 Italian and 12 Swedish sporadic patients with idiopathic CIPO were included in the study (eight males and 25 females; mean age: 38.6+/−16.6 years). In Table 1 the major clinical characteristics of these patients are described. 500 Turkish controls were recruited at the Universities of Ankara and Istanbul; 240 controls of European ancestry were recruited at the University of Bologna. All data from patients and controls, including the informed consents, were handled in accordance with local ethical committee's approved protocols and in compliance with the Helsinki declaration.

High-Throughput SNP genotyping and Whole Exome Sequencing Analysis

A detailed description of the SNP genotyping and whole exome sequencing analyses is reported in Supplementary materials. Variant detection and genotyping were annotated with the SeattleSeq137 Annotation Server.

RAD21 mutation screening in idiopathic CIPO cases

Genomic DNA extracted from peripheral blood was amplified as reported in Supplementary materials.

RAD21 cDNA transfection into HEK293 cells

3×10^5 HEK293 cells were plated for transfection of the different plasmids using liposomes as described in Supplementary materials.

Gene expression analysis

Total RNA from 1.5 ml fresh blood was extracted with the QIAGEN Blood Total RNA kit (QIAGEN, Venlo, Limburg, Netherlands). Total RNA from lymphoblastoid or transfected cells was extracted with RNeasy kit (QIAGEN). Real-time quantitative RT-PCR was performed as reported in Supplementary materials.

Zebrafish functional assays

To determine the effect of *rad21a* suppression in zebrafish embryos, a splice blocking morpholino was designed as described in Supplementary materials. A published *ret* MO was used.[18] To measure *rad21a* MO efficiency, total mRNA was extracted from control and MO

injected embryos, reverse-transcribed and the site targeted by the MO was PCR amplified (Supplementary Figure 1). *runx1* expression analysis and enteric nervous system characterization are reported in Supplementary materials.

Microgavage

Control and rad21 MO injected embryos were developed to 5dpf. Zebrafish larvae were anesthetized in Tricaine (Sigma), mounted in 3% methylcellulose and injected with fluorescent beads into the mouth as described.[19]

Electromobility shift assay (EMSA)

2×10^6 LCLs were processed for nuclear extract preparation as described in Supplementary materials.

Immunoprecipitation and western blotting

2×10^6 LCLs were used for immunoprecipitation assays. Crude sera of patients were diluted in PBS. Serial dilutions for cases and controls were performed (1:5, 1:10, 1:100, Supplementary Figure 2A). Immunoprecipitation and western blotting were performed as reported in Supplementary materials.

Immunohistochemistry

Immunohistochemistry was performed as reported in Supplementary materials. Incubations with the corresponding blocking peptides or with the secondary antibodies only were performed as negative controls (Supplementary Figure 2B, C).

Quantitative evaluation of ganglion cells

Quantitative evaluation of neuron number in myenteric and submucosal ganglia was performed according to[20] (see Supplementary materials).

Statistical analysis

Case-control association study for SNP rs72105712 was performed using Haploview 4.0 (http://www.broadinstitute.org/scientific-community/science/programs/medical-and-population-genetics/haploview/). Statistical analysis of quantitative differences was performed using the Student's t-test from the GraphPad package (http://graphpad.com/quickcalcs/). Fluorescent cell count was performed with ImageJ (http://rsbweb.nih.gov/ij); χ^2 tests were calculated using the dedicated option from GraphPad.

Results

Identification of a novel RAD21 mutation in CIPO

We performed a combined single nucleotide polymorphism (SNP)-genotyping/next generation-sequencing approach in a consanguineous CIPO pedigree of Turkish origin (Figure 1A), where we previously mapped a linkage locus with a multipoint LOD score=5.019. [14] High-throughput SNP-genotyping in the family and detection of Runs of Homozygosity (ROH) by PLINK (http://ngu.mgh.harvard.edu/~purcell/plink/) confirmed

the locus,[14] by identifying two regions of extended homozygosity: 91,878,147-113,307,176; 116,713,296-124,956,205 (Supplementary Table 1). We then performed WES on genomic DNA from two affected individuals (IV-9 and IV-11, Figure 1A). We filtered data for variants that were a) homozygous in our patients; b) rare (MAF <1%) in public databases (EVS, dbSNP); and c) predicted computationally to be pathogenic. We found a single variant fulfilling all these conditions inside our linkage interval on chromosome 8 (Figure 1; Supplementary Figure 3A). This homozygous allele affects the coding change c. 1864 G>A in *RAD21* (NM_006265.2), and is predicted to generate a missense substitution p.622 Ala>Thr (Figure 1B). Mutation Taster (http://www.mutationtaster.org/) and PolyPhen-2 (http://genetics.bwh.harvard.edu/pph2/)[21] analysis predicted this change to be "disease causing" and "damaging", respectively (Mutation Taster p= 0.9999; PolyPhen-2 HumDiv score: 0.999, sensitivity: 0.14; specificity: 0.99; HumVar score: 0.993; sensitivity: 0.47; specificity: 0.96), and the variant was absent from public databases (dbSN: www.ncbi.nlm.nih.gov/SNP/, 1000 Genomes: www.1000genomes.org/, ESP: http://evs.gs.washington.edu/EVS/) and from 1000 control chromosomes of Turkish origin analyzed by our group. To test the candidacy of this allele, we performed segregation analysis on all available family members: all three affected sibs carried the change in a homozygous state and all carriers of the risk haplotype (including the parents) were heterozygous (Figure 1A).

To evaluate whether *RAD21* mutations were also prevalent in other idiopathic CIPO cases, we screened 21 Italian and 12 Swedish individuals with pseudo-obstruction, defined by clinical, manometric and radiological examination (Table 1). We did not identify any mutation in *RAD21* coding region, although a 1bp-indel was detected with high frequency in the upstream region (m.a.f= 0.364; g.11788122-11788123 ins(C)); rs72105712 (dbSNP137)). Since no allele frequencies were known for this SNP, we investigated the frequency in a control group of European ancestry (N= 240); we found no differences between cases and controls (m.a.f.= 0.36 in cases; 0.34 in controls; χ^2= 0.08, p-value= 0.77).

Mutant RAD21 p.622 Ala>Thr alters RUNX1 expression

To test the candidacy of *RAD21* further, we evaluated its expression in blood and lymphoblastoid cell lines (LCLs) obtained from one homozygous patient and several controls, including one unaffected wild-type brother. Real-time quantitative RT-PCR (qRT-PCR) showed that *RAD21* expression in the affected individual was comparable to that in controls, either in blood (Supplementary Figure 3B) or in LCL cDNA (Supplementary Figure 3C). The mutant protein was also expressed in LCLs in amounts comparable to wild-type cells (Supplementary Figure 3D; upper panel). Likewise, testing the interaction of RAD21 with SMC1, one of its known partners,[22] co-immunoprecipitation experiments showed that the mutant protein still retains SMC1-binding activity (Supplementary Figure 3D, middle panel).

Since one of the main target genes activated by RAD21 is *RUNX1*[23,24] we investigated whether mutated RAD21 could hamper its transcription activity: indeed, the affected individual's LCLs showed significantly reduced *RUNX1* expression compared to controls (Figure 1C). Similarly, transfection of mutant *RAD21* cDNA in HEK293 cells and

subsequent RT-qPCR revealed a significant decrease in *RUNX1* expression (p=0.0028, Student's t-test) compared to cells transfected with wild-type *RAD21* cDNA (Supplementary Figure 3E).

Rad21a suppression causes downregulation of runx1 expression and loss of enteric neurons in vivo

To test the hypothesis that RAD21 is necessary for enteric development and to assay the pathogenic potential of the newly discovered allele in a physiologically relevant *in vivo* system, we investigated RAD21 in zebrafish development.

Given our *in vitro* observations on the role of RAD21 on *RUNX1* expression and its downregulation in patient's cells, we asked whether *RAD21* can replicate this defect *in vivo* and whether the patient's mutation has the expected effect. We identified (by reciprocal BLAST) the sole ortholog of *RAD21* and we injected zebrafish embryos with a *rad21a* splice blocking morpholino (MO) (at 1–2 cell stage, Supplementary Figure 2A,B). Embryos were fixed at 14hpf (hours post fertilization) and stained with a *runx1* probe. During zebrafish development, *runx1* is expressed in the posterior lateral plate mesoderm (PLM). We observed defects in *runx1* expression patterns recapitulating prior studies,[23,24] with *runx1* expression either partially or completely absent in *rad21a* morphants (Figures 2A–C). *Runx1* expression was rescued by co-injection of MO with human WT *RAD21 mRNA*. In contrast, co-injection of MO and mRNA encoding the p.622 Thr allele was not able to rescue *runx1* expression, indicating that the RAD21 mutation has a loss-of-function effect *in vivo* (Figure 2D).

To test whether we could recapitulate the CIPO phenotype seen in *RAD21* mutant patients, including a severe impairment of gut motility and marked hypoganglionosis,[14] we characterized the zebrafish gut. Subsequent to MO injection, embryos were allowed to develop to 5dpf, at which time the digestive system has developed.[25] Notably, we saw no appreciable *runx1* expression in the gut at this stage of development (data not shown), suggesting an earlier onset of the enteric phenotype. Control and MO embryos were fed fluorescent beads through microgavage, a technique that allows to determine the rate of intestinal motility as a function of time.[19] After eight hours post bead injection (hpi), embryos were divided into 1–4 zones based on anatomical landmarks (Figure 3A) and the presence of fluorescence in each segment was scored. Consistent with the CIPO phenotype, *rad21a* morphants showed delayed food transit along the gut (Figure 3B). Moreover, staining of enteric neurons along the gut with antibodies against HuC/D showed a significant depletion of enteric neurons (Figure 3C). Quantitative analysis of the zebrafish gut (Figure 3D) at 4 (upper panel) and 5 (lower panel) dpf stages revealed that *rad21* morphants had a marked reduction of HuC/D-immunolabeled enteric neurons compared to controls, suggesting a neurogenic cause of the observed motility defects.

Notably, previous reports on *rad21a* morphants and *rad21*^{nz171} mutants have shown significantly reduced expression of *ascl1a*,[26] a neuronal marker. Ascl1 is also a transcription factor required for the development of serotonergic neurons.[26] An ASCL1 mutation has been reported previously in Haddad syndrome, a condition encompassing congenital central hypoventilation syndrome and Hirschsprung disease (MIM 209880).

These data, the similarity of *rad21a* morphants to the hypoganglionic phenotype observed in a mouse model for the *ret* mutation C620R[27,28]raised the possibility that RAD21 and RET might act synergistically during gut neurogenesis. We therefore performed epistasis analysis by co-injecting *rad21a* and *ret* MOs at subeffective doses, at which each MO alone was indistinguishable from control embryos. We observed strong epistasis on the innervation of the gut; co-injection of the two genes phenocopied the phenotype of high dose *rad21* MOs (Figures 3E, F). At the same time, overexpression of RET did not rescue *rad21* morphants, or vice versa, suggesting that the two genes act on the same process but not directly in the same pathway. This observation is consistent with previous studies that showed RET to be induced by NGF in a runx1-independent manner.[29]

The mutant RAD21 p.622 Ala>Thr does not bind to RAD21-binding elements in Apolipoprotein B promoter

Recent data have shown that RAD21/CTCF binding sites are present in the apolipoprotein A1/C3/A4/A5 gene cluster on chromosome 11 and that altered binding of these factors to these sites dysregulates apolipoprotein expression.[30] We therefore performed electromobility shift assay (EMSA) experiments to test whether the mutant RAD21 protein could retain its binding affinity for the above-mentioned sites, in particular for the AC2 site. [30] We observed no differences between the nuclear extracts from wild-type and mutant LCLs in binding to this site (Supplementary Figure 3F). Next, we investigated if the nuclear extracts from wild-type and mutant LCLs could show differences in binding to human *APOB* promoter [31]. *In silico* analysis with MatInspector identified two binding sites for RAD21/CTCF (hAPOB_c1, chr2:21,267,137-21,267,173, matrix score: 0.862; hAPOB_c2, chr2:21,266,910-21,266,945, matrix score: 0.807) which maps to the two regulatory regions of the proximal *APOB* promoter[31]. EMSA assays performed with probes corresponding to the two sites showed a specific shift only in the presence of wild-type nuclear extracts (Figure 4A). Moreover, specific supershifts with an anti-RAD21 antibody were detectable only in wild-type, but not in mutant, nuclear extracts (Supplementary Figure 4A). Transfection of the plasmids carrying either wild-type or mutant RAD21 cDNAs in frame with the DDK-epitope, in HEK293 cells, and subsequent RT-qPCR analysis of *APOB* expression revealed that wild-type RAD21 overexpression reduced *APOB* levels compared to the empty vector ($p=0.0098$; Student's t-test). In contrast, overexpression of the mutant protein had no effect, similarly to the empty-vector transfections (Figures 4B,C). These data suggest that RAD21 might act as a repressor of APOB.

Apolipoprotein B (APOB) is overexpressed in CIPO patients

APOB transcript generates two different proteins, APOB48 and APOB100 isoforms, both present in serum.[17] Since our data suggested a RAD21-regulated expression of APOB, we analyzed sera from the CIPO patient homozygous for *RAD21* mutation (IV-9), and from wild-type controls. We detected an elevated expression of APOB48 in the patient, whereas no significant differences could be appreciated for APOB100 (Figure 5A and Supplementary Figure 5A). To understand whether APOB overexpression was unique to this patient or whether it might represent a more generalized phenomenon, we evaluated sera from RAD21 mutation-negative idiopathic CIPO patients and from control subjects. APOB48 showed an increase in CIPO patients (Figure 5B and Supplementary Figure 5B). Moreover, compared

to CIPO, sera derived from 12 patients with functional bowel disease, namely seven diarrhea-predominant IBS (IBS-D), four constipation predominant IBS (IBS-C) and one with alternating bowel IBS (IBS-C/D), did not show APOB48 overexpression (Figure 5C and Supplementary Figure 5C). Furthermore, western blot analysis on the sera of patients with other gastrointestinal disorders, i.e. anorexia nervosa and mechanical intestinal obstruction, did not identify any APOB48 increase (F. Bianco et al., data not shown).

Immunohistochemical analysis of gut biopsies (mainly ileum) of sporadic CIPO patients revealed APOB48 expression in myenteric neurons and in cells of the *lamina propria*, reminiscent of immunocytes (Figure 5). Consistent with the results obtained in the sera, the APOB48 signal was increased markedly in the biopsies of CIPO cases compared to controls and IBS cases (Figures 5D i-iv-vii). The quantitative analysis of immunolabeled cells in the *lamina propria* of eight CIPO patients (five Italian and three Swedish) indicated a significant increase in the number of APOB48-positive cells compared to the other individuals (controls n=3;IBS patients n=3) (32.9±9.2% vs 7.2±2.5% cases vs controls; p=0.0012, Student' t test; 32.9±9.2% vs 5.6±1.5% CIPO cases vs IBS cases; p=0.0008; CIPO cases (8) vs all (6), p=0.0001; Figures 5Dv-vi-vii). In addition, quantitative analysis performed in the gut biopsies of sporadic CIPO patients with a marked increased in APOB48 revealed a significant reduction in the number of neuron specific enolase (NSE)-labeled myenteric ganglion cell bodies / gaglion compared to control specimens (CIPO cases 22.71± 8.10 vs controls 48.65±13.80; p-value=0.0039, Student's t-test; Figure 5E). No significant differences were observed for neurons in the submucosal plexus between CIPO cases and controls (CIPO cases 5.61 ± 0.39 vs controls 8.36 ±2.96; p-value=0.1079, Student's t-test). We observed RAD21 staining in multiple tissues and throughout different components of the gut, as shown previously (www.proteinatlas.org), although no differences were appreciated between CIPO and controls (Supplementary Figure 6A i-iv). Expression of APOBEC1, the gut-specific RNA editing enzyme responsible of the formation of APOB48 isoform, was also investigated; we observed similar immunostaining in control and CIPO tissue biopsies (Supplementary Figure 6B i-ii).

Discussion

This study provides *in vitro* and *in vivo* evidence that a novel homozygous mutation in *RAD21* is associated with a syndromic form of CIPO. RAD21 is part of the cohesin complex, forms a physical link between SMC1/SMC3 and STAG subunits, and controls sister chromatid pairing and unpairing during cell replication. [32] RAD21 is also a transcriptional regulator that binds to many sites in the genome. [33] In concordance with the key role(s) of RAD21 in regulating cell division, altered expression and somatic loss-of-function mutations have been reported in different cancers.[34,35] Furthermore, heterozygous germline mutations in cohesin subunits, i.e. RAD21, SMC1, STAG, or in regulators of cohesin, e.g. NIPBL, cause a broad spectrum of disorders referred to as cohesinopathies (namely Cornelia de Lange syndrome, CdLS, OMIM 122470), characterized by facial dysmorphisms, growth retardation, developmental delay and/or intellectual disability, and multiorgan involvement, including musculoskeletal malformations ranging from brachyclinodactyly to severe reduction defects.[36–39]

We observed a similar loss-of-function phenotype for two missense CdL mutations (p. 376Pro>Arg, p.585Cys>Arg) and for our CIPO variant in RAD21 (p.622Ala>Thr). However, in the consanguineous family studied herein the heterozygous carriers of the *RAD21* mutation did not show sign of CdLS.[14] Previously described patients with CdLS and different *RAD21* heterozygous mutations did not show gastrointestinal abnormalities such as CIPO.[32,40] It is worth noting that the mutations observed in CdLS and in our CIPO patients map to different RAD21 domains, potentially suggesting that specific mutational mechanisms in RAD21 can lead to different clinical entities in humans. Consistent with this notion, the CIPO-causing mutations do not appear to abolish the ability of RAD21 to bind to SMC1, whereas it does attenuate its transcriptional repressive role of other targets, such as APOB. Recently, however, a mutation in *SGOL1*, another cohesin protein, has been associated to severe gut and cardiac dysrhythmia in the absence of other congenital abnormalities or cohesinopathies.[13]

RAD21 plays an important role in the development, survival and maintenance of epithelial cells and neurons of the gastrointestinal tract and mice heterozygous for a *Rad21* null mutation exhibit gastrointestinal defects following X-ray irradiation.[41] Our zebrafish studies suggest that *rad21* is essential for enteric neuron development: *rad21a* morphants recapitulate the CIPO phenotype, as they show a delayed transit along the gut and a significant depletion of enteric neurons. This latter finding is reminiscent of an enteric neuronal hypoganglionic phenotype observed in heterozygous $ret^{C620R/+}$ mice[16] and shares similarities with the histopathology of some CIPO patients.[14,27,28] The similarity of the *rad21* suppression phenotype in zebrafish to the neuronal defects of heterozygous $ret^{C620R/+}$ mice prompted us to test whether those two genes might interact genetically. We showed that RET and RAD21 interact epistatically during differentiation or maintenance of enteric neurons. However, the failure of the two genes to rescue the gut innervation phenotype suggests that they activate different molecular pathways.

Our previous studies identified Apolipoprotein B (*Apob*) as a target of RET signaling in Neuro2a cells, a murine model of enteric nervous system development. Moreover, in $ret^{+/C620R}$ mice that have an enteric neuronal hypoganglionic phenotype[16] reminiscent of the histopathology observed in some CIPO patients,[27,29] *Apob* was markedly overexpressed. APOB is a major constituent of the plasma lipoprotein, and in mammals is synthesized in two different tissues, i.e. liver and intestine. Two different proteins derive from the APOB transcript by a RNA-editing enzyme, APOBEC1: the full-lenght APOB100, a large protein of 512 kDa synthesized by the liver (which does not express APOBEC1), essential for triglyceride-rich VLDL formation; and the gut-specific isoform APOB48, formed via the RNA-editing process and co-linear with the N-terminal half of APOB100. APOB48 has a key role in chylomicron assembly and transport in the intestine.[17]

APOB expression is regulated by a strong promoter in the proximal upstream region, containing several positive regulatory elements, including one within the noncoding exon 1, but also a negative regulatory element between bases −261 and −129.[31] In this study we identified two RAD21-binding sites in APOB proximal promoter, i.e. one overlapping the negative element, and the other partially overlapping the exon 1 positive regulatory element. Only nuclear extracts from wild-type cells form a specific complex with either region,

whereas no complex is observed in the presence of mutant RAD21. This suggests that RAD21 may act as a repressor of APOB transcription, associating to its negative regulatory element and competing with the transcriptional activators that bind to positive regulatory element.

Finally, we found that, compared to controls, gut-specific APOB48[17] levels were increased in the serum of the RAD21-mutated CIPO patient. Interestingly, sera from the sporadic CIPO patients, negative for RAD21 mutations, also showed consistently elevated APOB48 levels as compared to either IBS patients or healthy controls. We observed a variable expression of APOB100 in both controls and CIPO patients, in line with the fact that its regulation depends on different factors, including cholesterol and insulin levels.[42] Notably, CIPO patients did not show evidence of altered lipid metabolism, i.e. total cholesterol and HDL levels were within the normal range (Supplementary Table 2).

APOB48 overexpression was further corroborated by the data on gut biopsies of CIPO patients: compared to controls, APOB48 immunoreactivity was significantly increased in cells (with morphological features of immunocytes) distributed throughout the *lamina propria* and in myenteric neurons of CIPO patients. Interestingly, a recent study identified a specific neuron-macrophage crosstalk in regulating gut motility.[43] These data bear implications to the pathogenesis of functional bowel disorders, such as IBS. However, our study did not show any change in APOB expression in patients with IBS, suggesting that other molecular pathways can be also involved in patients with a more prominent gut dysfunction such as those with CIPO.

Furthermore, we found a significant decrease in the mean number of myenteric neurons / ganglion in CIPO tissues exhibiting a high APOB immunoreactivity. This finding is reminiscent of severe hypoganglionosis[14] in the patients who were found to carry the RAD21 p.622Ala>Thr homozygous mutation in this study.

Based on our data, APOB48 expression (at serum and tissue level) was homogeneously increased in sporadic and familial CIPO and therefore making a possible correlation between this marker and the degree of neuronal loss / symptom severity undetectable. Further studies are eagerly awaited to clarify whether the correlation between APOB expression levels and neuronal / clinical CIPO phenotype exists.

It is currently unclear the pathophysiological significance of the generalized APOB overexpression observed in sporadic CIPO, where no mutation of RAD21 were identified. Our previous studies suggested a role for APOB in the molecular pathways required for enteric neuron development and survival.[16] Therefore, APOB48 increase may be activated as a compensatory effect to an abnormal / defective enteric nervous system occurring in CIPO. We still do not know the precise temporal origin of the defect that leads to CIPO in patients with RAD21 mutations. The observed transcriptional downregulation of *runx1*, which is likely relevant in early neuronal progenitors, possibly in the crest, argues for a migratory defect. At the same time, the observed loss of APOB suppression might be more relevant to neuronal progenitors in the gut itself (Figure 6). Further studies of patients and conditional mouse mutants will be required to understand the potential relative contribution

of different sites to CIPO pathology. Likewise, further research will be required to elucidate the factors contributing to the specific APOB48 overexpression and its clinical value in the management of CIPO patients. Nonetheless, our data inform the molecular aspects underlying the pathogenesis of CIPO and lead to the identification of a candidate biomarker, namely APOB48 overexpression, for this severe, disabling gut dysmotility disorder.

Supplementary Material

Refer to Web version on PubMed Central for supplementary material.

Acknowledgements

We thank Dr. M. Vargiolu for helpful suggestions and critical reading. N. K. is a Distinguished Brumley Professor.

Grant support: This work was supported by FP7-EU grant n° 223692 “CHERISH” to G. R., by NIH grant n° 1U54HG006493 to M. B. and P50DK096415 to N.K., by Ricerca Finalizzata RER2009 (Ita-MNGIE), Ministry of Health, and the Italian Ministry of University and Research (PRIN/COFIN 2009MFSXNZ_002) to R. De G. R. De G. is also the recipient of grants from ‘Fondazione del Monte di Bologna e Ravenna’, Bologna, Italy.

Abbreviations used in this paper

CIPO	Chronic intestinal pseudo-obstruction
APOB48	Apolipoprotein B48
WES	Whole exome sequencing
EMSA	electromobility shift assays
FLNA	filamin A
ACTG	actin G2
TYMP	thymidine phosphorylase
POLG1	polymerase gamma
MGS	Mungan syndrome
IBS	Irritable Bowel Disease
ROH	Runs Of Homozygosity
BWA	Burrows-Wheeler Aligner; v0.6.2
GATK	Genome Analysis Toolkit
dpf	days post fertilization
SNP	single nucleotide polymorphism
LCLs	lymphoblastoid cell lines
qRT-PCR	Real-time quantitative RT-PCR
MO	morpholino
hpf	hours post fertilization

hpi	post bead injection
nNOS	nitric oxide synthase
IBS-D	diarrhea-predominant IBS
IBS-C	constipation predominant IBS
CdLS	Cornelia de Lange syndrome
AF	activity front(s)
BUPA	bursts of uncoordinated phasic activity
EN	enteral nutrition
ICC	interstitial cells of Cajal
PPN	partial parenteral nutrition
TPN	total parenteral nutrition
SPUPA	sustained periods of uncoordinated phasic activity

References

1. Amiot A, Joly F, Alves A, et al. Long-term outcome of chronic intestinal pseudo-obstruction adult patients requiring home parenteral nutrition. Am J Gastroenterol. 2009; 104:1262–1270. [PubMed: 19367271]
2. Lindberg G, Iwarzon M, Tornblom H. Clinical features and long-term survival in chronic intestinal pseudo-obstruction and enteric dysmotility. Scand J Gastroenterol. 2009; 44:692–699. [PubMed: 19308797]
3. Stanghellini V, Cogliandro R, De Giorgio R, et al. Natural history of chronic idiopathic intestinal pseudo-obstruction in adults: a single center study. Clin Gastroenterol Hepatol. 2005; 3:449–458. [PubMed: 15880314]
4. De Giorgio R, Sarnelli G, Corinaldesi R, et al. Advances in our understanding of the pathology of chronic intestinal pseudo-obstruction. Gut. 2004; 53:1549–1552. [PubMed: 15479666]
5. De Giorgio R, Seri M, van Eys G. Deciphering chronic intestinal pseudo-obstruction: do mice help to solve the riddle? Gastroenterology. 2007; 133:2052–2055. [PubMed: 18054578]
6. Stanghellini V, Cogliandro RF, De Giorgio R, et al. Chronic intestinal pseudo-obstruction: manifestations, natural history and management. Neurogastroenterol Motil. 2007; 19:440–452. [PubMed: 17564625]
7. Mann SD, Debinski HS, Kamm MA. Clinical characteristics of chronic idiopathic intestinal pseudo-obstruction in adults. Gut. 1997; 41:675–681. [PubMed: 9414977]
8. Clayton-Smith J, Walters S, Hobson E, et al. Xq28 duplication presenting with intestinal and bladder dysfunction and a distinctive facial appearance. Eur J Hum Genet. 2009; 17:434–443. [PubMed: 18854860]
9. Gargiulo A, Auricchio R, Barone MV, et al. Filamin A is mutated in X-linked chronic idiopathic intestinal pseudo-obstruction with central nervous system involvement. Am J Hum Genet. 2007; 80:751–758. [PubMed: 17357080]
10. Lehtonen HJ, Sipponen T, Tojkander S, et al. Segregation of a missense variant in enteric smooth muscle actin gamma-2 with autosomal dominant familial visceral myopathy. Gastroenterology. 2012; 143:1482–1491. e3. [PubMed: 22960657]
11. Nishino I, Spinazzola A, Hirano M. Thymidine phosphorylase gene mutations in MNGIE, a human mitochondrial disorder. Science. 1999; 283:689–692. [PubMed: 9924029]

12. Giordano C, Powell H, Leopizzi M, et al. Fatal congenital myopathy and gastrointestinal pseudo-obstruction due to POLG1 mutations. Neurology. 2009; 72:1103–1105. [PubMed: 19307547]
13. Chetaille P, Preuss C, Burkhard S, et al. Mutations in SGOL1 cause a novel cohesinopathy affecting heart and gut rhythm. Nat Genet. 2014; 46:1245–1249. [PubMed: 25282101]
14. Deglincerti A, De Giorgio R, Cefle K, et al. A novel locus for syndromic chronic idiopathic intestinal pseudo-obstruction maps to chromosome 8q23-q24. Eur J Hum Genet. 2007; 15:889–897. [PubMed: 17487221]
15. Mungan Z, Akyuz F, Bugra Z, et al. Familial visceral myopathy with pseudo-obstruction, megaduodenum, Barrett's esophagus, and cardiac abnormalities. Am J Gastroenterol. 2003; 98:2556–2560. [PubMed: 14638363]
16. Evangelisti C, Bianco F, Pradella LM, et al. Apolipoprotein B is a new target of the GDNF/RET and ET-3/EDNRB signalling pathways. Neurogastroenterol Motil. 2012; 24:e497–e508. [PubMed: 22897442]
17. Black DD. Development and physiological regulation of intestinal lipid absorption. I. Development of intestinal lipid absorption: cellular events in chylomicron assembly and secretion. Am J Physiol Gastrointest Liver Physiol. 2007; 293:G519–G524. [PubMed: 17495031]
18. Heanue TA, Pachnis V. Ret isoform function and marker gene expression in the enteric nervous system is conserved across diverse vertebrate species. Mech Dev. 2008; 125:687–699. [PubMed: 18565740]
19. Cocchiaro JL, Rawls JF. Microgavage of zebrafish larvae. J Vis Exp. 2013; 72:e4434. [PubMed: 23463135]
20. Ganns D, Schrodl F, Neuhuber W, et al. Investigation of general and cytoskeletal markers to estimate numbers and proportions of neurons in the human intestine. Histol Histopathol. 2006; 21:41–51. [PubMed: 16267786]
21. Adzhubei IA, Schmidt S, Peshkin L, et al. A method and server for predicting damaging missense mutations. Nat Methods. 2010; 7:248–249. [PubMed: 20354512]
22. Panigrahi AK, Zhang N, Otta SK, et al. A cohesin-RAD21 interactome. Biochem J. 2012; 442:661–670. [PubMed: 22145905]
23. Horsfield JA, Anagnostou SH, Hu JK, et al. Cohesin-dependent regulation of Runx genes. Development. 2007; 134:2639–2649. [PubMed: 17567667]
24. Marsman J, O'Neill AC, Kao BR, et al. Cohesin and CTCF differentially regulate spatiotemporal runx1 expression during zebrafish development. Biochim Biophys Acta. 2014; 1839:50–61. [PubMed: 24321385]
25. Ng AN, de Jong-Curtain TA, Mawdsley DJ, et al. Formation of the digestive system in zebrafish: III. Intestinal epithelium morphogenesis. Dev Biol. 2005; 286:114–135. [PubMed: 16125164]
26. Pattyn A, Simplicio N, van Doorninck JH, et al. Ascl1/Mash1 is required for the development of central serotonergic neurons. Nat Neurosci. 2004; 7:589–595. [PubMed: 15133515]
27. Carniti C, Belluco S, Riccardi E, et al. The Ret(C620R) mutation affects renal and enteric development in a mouse model of Hirschsprung's disease. Am J Pathol. 2006; 168:1262–1275. [PubMed: 16565500]
28. Yin L, Puliti A, Bonora E, et al. C620R mutation of the murine ret proto-oncogene: loss of function effect in homozygotes and possible gain of function effect in heterozygotes. Int J Cancer. 2007; 121:292–300. [PubMed: 17372903]
29. Luo W, Wickramasinghe SR, Savitt JM, et al. A hierarchical NGF signaling cascade controls Ret-dependent and Ret-independent events during development of nonpeptidergic DRG neurons. Neuron. 2007; 54:739–754. [PubMed: 17553423]
30. Mishiro T, Ishihara K, Hino S, et al. Architectural roles of multiple chromatin insulators at the human apolipoprotein gene cluster. Embo J. 2009; 28:1234–1245. [PubMed: 19322193]
31. Carlsson P, Bjursell G. Negative and positive promoter elements contribute to tissue specificity of apolipoprotein B expression. Gene. 1989; 77:113–121. [PubMed: 2501159]
32. Deardorff MA, Wilde JJ, Albrecht M, et al. RAD21 mutations cause a human cohesinopathy. Am J Hum Genet. 2012; 90:1014–1027. [PubMed: 22633399]
33. Parelho V, Hadjur S, Spivakov M, et al. Cohesins functionally associate with CTCF on mammalian chromosome arms. Cell. 2008; 132:422–433. [PubMed: 18237772]

34. Cuadrado A, Remeseiro S, Gomez-Lopez G, et al. The specific contributions of cohesin-SA1 to cohesion and gene expression: implications for cancer and development. Cell Cycle. 2012; 11:2233–2238. [PubMed: 22617390]

35. Kon A, Shin LY, Minamino M, et al. Recurrent mutations in multiple components of the cohesin complex in myeloid neoplasms. Nat Genet. 2013; 45:1232–1237. [PubMed: 23955599]

36. de Lange C. Sur un type nouveau de degenerescence (typus Amstelodamensis). Arch. Med. Enfants. 1933; 36:713–719.

37. Ireland M, Donnai D, Burn J. Brachmann-de Lange syndrome. Delineation of the clinical phenotype. Am J Med Genet. 1993; 47:959–964. [PubMed: 8291539]

38. Jackson L, Kline AD, Barr MA, et al. de Lange syndrome: a clinical review of 310 individuals. Am J Med Genet. 1993; 47:940–6. [PubMed: 8291537]

39. Opitz JM. The Brachmann-de Lange syndrome. Am J Med Genet. 1985; 22:89–102. [PubMed: 3901753]

40. Minor A, Shinawi M, Hogue JS, et al. Two novel RAD21 mutations in patients with mild Cornelia de Lange syndrome-like presentation and report of the first familial case. Gene. 2014; 537:279–284. [PubMed: 24378232]

41. Xu H, Balakrishnan K, Malaterre J, et al. Rad21-cohesin haploinsufficiency impedes DNA repair and enhances gastrointestinal radiosensitivity in mice. PLoS One. 2010; 5:e12112. [PubMed: 20711430]

42. Watts GF, Ooi EM, Chan DC. Therapeutic regulation of apoB100 metabolism in insulin resistance in vivo. Pharmacol Ther. 2009; 123:281–291. [PubMed: 19490928]

43. Muller PA, Koscsó B, Rajani GM, et al. Crosstalk between muscularis macrophages and enteric neurons regulates gastrointestinal motility. Cell. 2014; 158:300–313. [PubMed: 25036630]

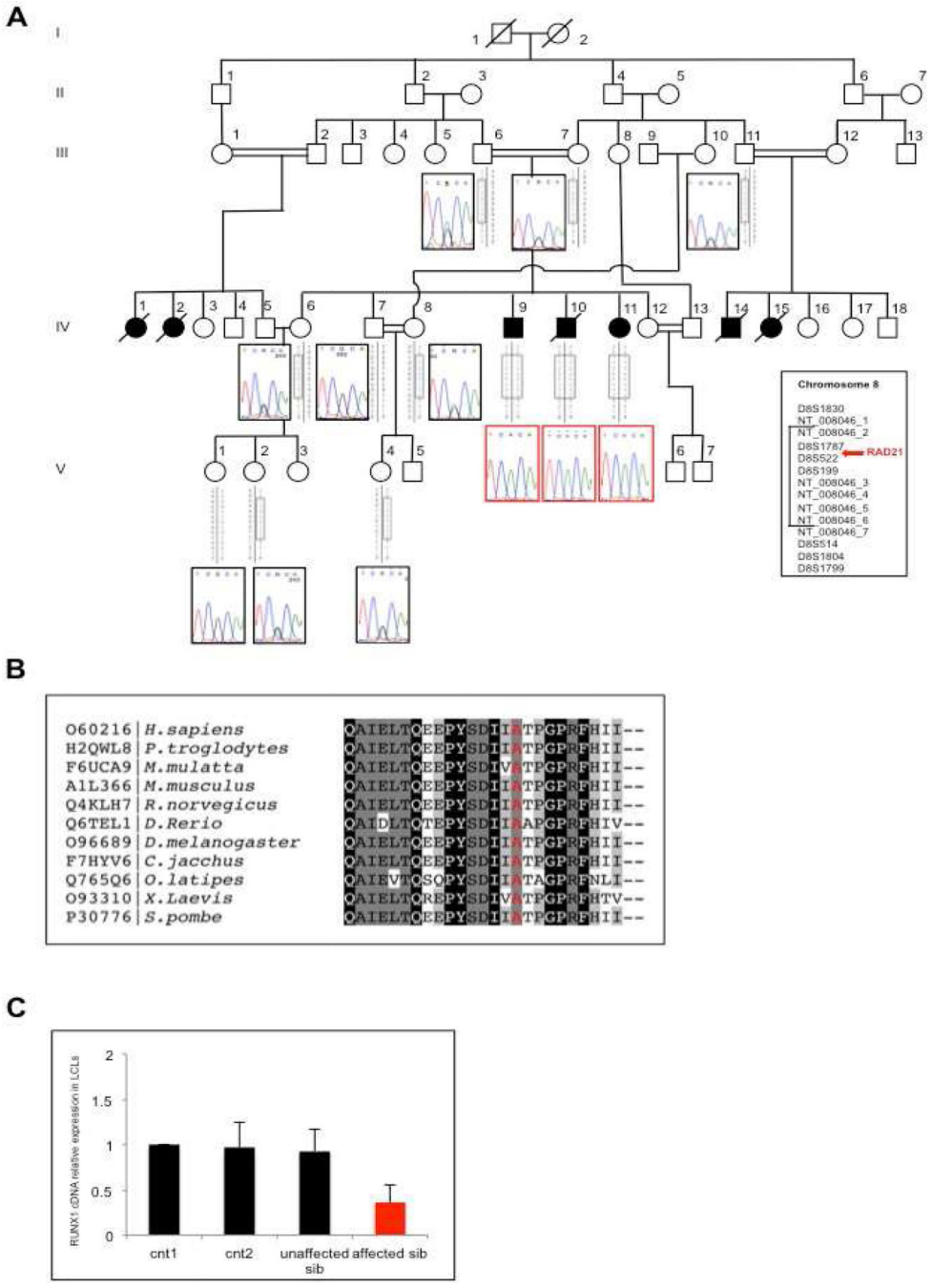

Figure 1. Identification of a novel homozygous mutation in RAD21

(**A**) Pedigree of the Turkish consanguineous family showing the segregation of the RAD21 mutation in the available members. For the homozygous patients, electropherograms are boxed in red. Grey boxes represent the haplotypes derived from microsatellite analysis. (**B**) RAD21 conservation across species surrounding the position p.622Ala (highlighted in red). (**C**) *RUNX1* expression in controls and patient's LCLs (IV-9).

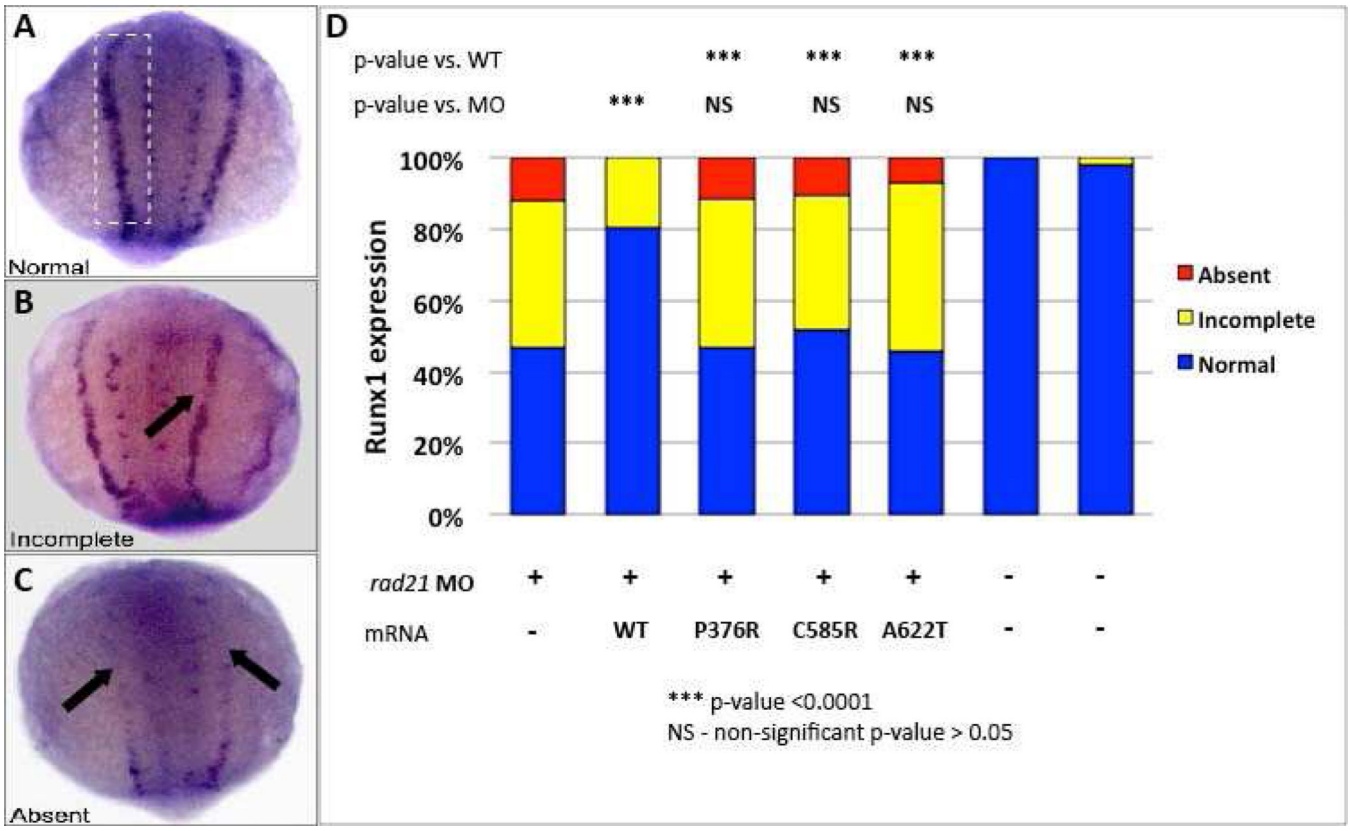

Figure 2. (A–D) RAD21 A622T affects *runx1* expression in zebrafish embryos

runx1 expression in the PLM in *rad21a* morpholino injected embryos rescued with wild type or mutants *RAD21*. Morpholino injected embryos were scored according to *runx1* expression in the PLM as normal (**A**), partial (**B**), or absent (**C**). *rad21a* morphants could be rescued by wild type human RAD21 mRNA, while mutations previously reported in patients with “cohesinopathy” (P376A, C585R) and A622T can not rescue this phenotype.

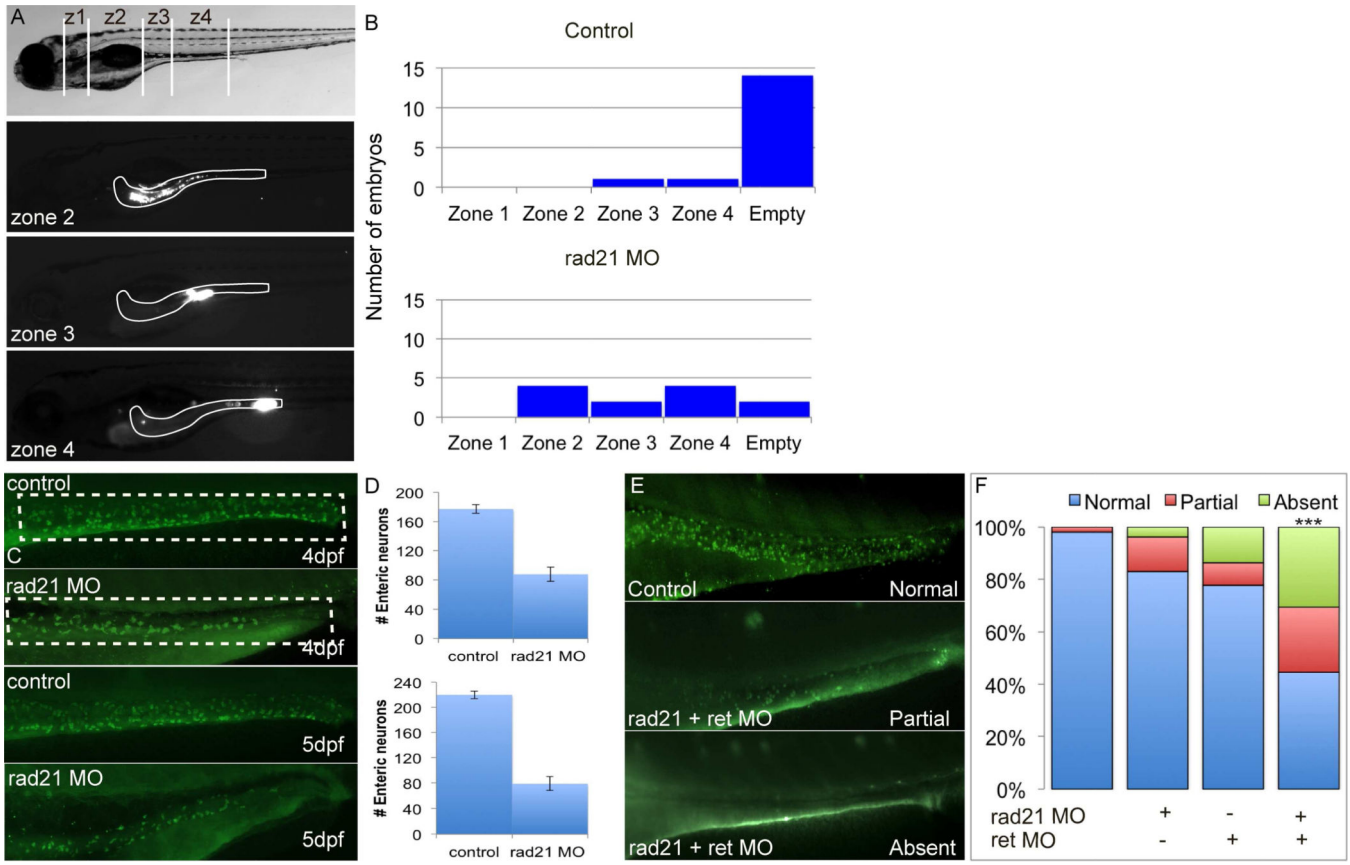

Figure 3. Gut dysmotility is caused by enteric neuronal loss in zebrafish embryos

To assess gut motility in zebrafish larvae, we injected fluorescent beads into the mouth and recorded the rate of gut motility versus time. (**A**) Lateral view of 5dpf zebrafish larvae. Representative images of injected larvae show (after eight hours post injection, hpi) fluorescent beads in different gut compartments (zone 1–4). (**B**) In control embryos, most of the fluorescent beads have exited the gut by 8hpi, while *rad21* MO injected embryos have reduced gut motility. (**C-D**) Compared to control larvae, *rad21* morphants have a significant reduction of enteric HuC/D immunoreactive neurons at 4dpf (**D**; upper panel) and 5dpf (**D**; lower panel). (**E**) *rad21* and *ret* interaction during the ENS development. Combination of suboptimal doses of *rad21* and *ret* MOs causes a significant decrease in HuC/D enteric neurons, while embryos injected with suboptimal doses of *rad21* MO or *ret* MO causes loss of HuC/D enteric neurons, not statistically significant (**F**).

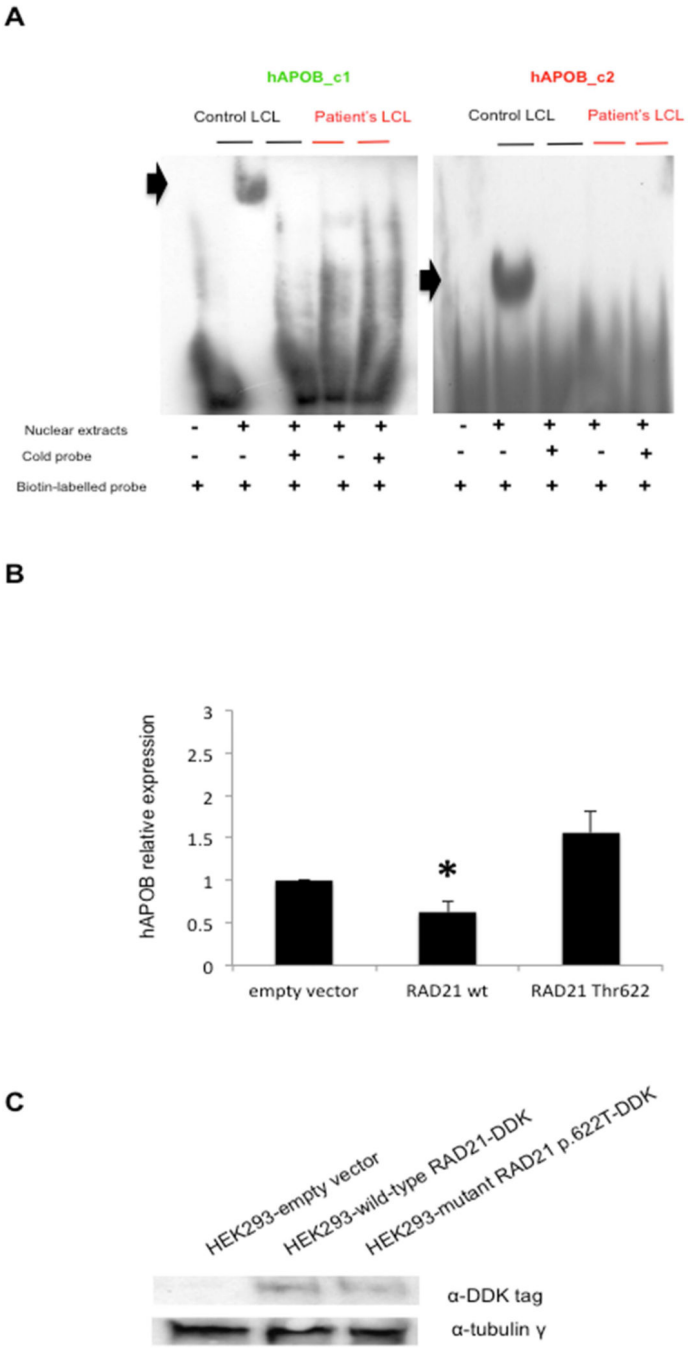

Figure 4. RAD21 regulates APOB overexpression

(**A**) EMSA on human APOB promoter containing two putative binding sites for RAD21: hAPOB_c1 (green), hAPOB_c2 (red). EMSA analysis for hAPOB_c1 and _c2 regions biotin-labelled probes: only the nuclear extracts from wild-type (control) LCL) show a specific gel-shift (black arrows). (**B**): RT-qPCR for *APOB* expression in HEK293 cells transfected either with empty, RAD21 wild-type, RAD21 mutant p.622 Thr vectors. Data represent the mean values of three independent transfection experiments. Bars represent the standard deviation; black asterisk indicates the significant p-value (see in text). (**C**) Western

blotting analysis showing the expression of recombinant wild-type and mutant RAD21 in frame with DDK tag in transfected HEK293.

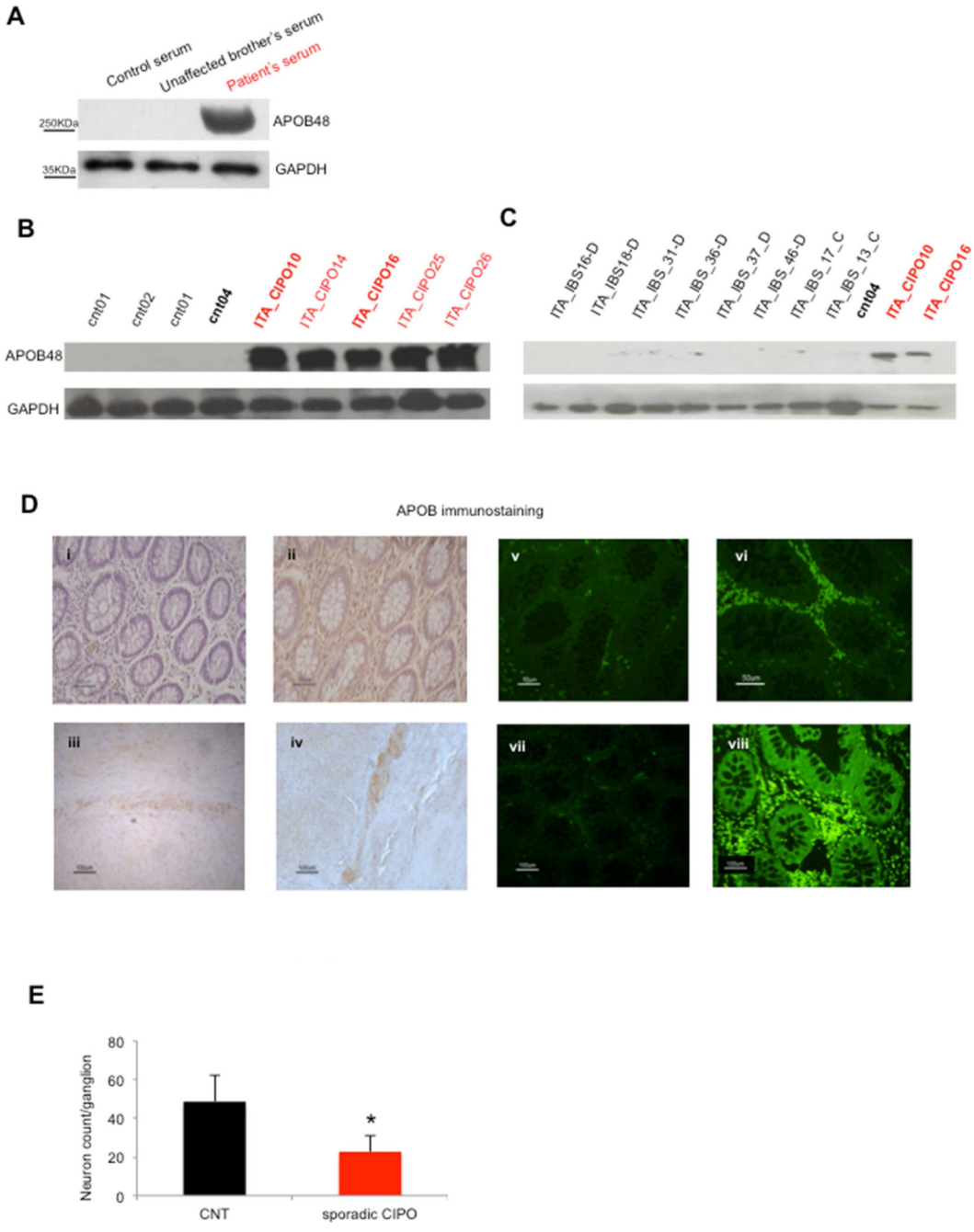

Figure 5. APOB overexpression is specific for CIPO patients

(**A**)Western blotting analysis showing APOB48 expression in the patient carrying the homozygous RAD21 mutation (third lane), compared to control sera (upper panel); GAPDH was used as internal loading control (lower panel). (**B**) Western blotting analysis showing APOB overexpression in the sera of CIPO patients compared to controls (upper panel). (**C**) Western blotting analysis for APOB48 in IBS samples *vs* controls (in black) and CIPO patients (in red). Samples loaded in duplicates/triplicates are marked in bold (as index of

reproducible blotting). IBS-C: constipation predominant irritable bowel syndrome; IBS-D: diarrhea predominant irritable bowel syndrome.

(**D**) Immunohistochemistry and immunofluorescence staining for APOB in controls (**D**-i, iii, v), IBS cases (**D**-vii) and CIPO patients (**D**-ii, iv, vi). Representative figures (**D**-i, ii) illustrate immunostaining of immunocyte-like cells distributed throughout the mucosa, including the *lamina propria* and the myenteric plexus (**D**-iii, iv). Note that the density of APOB immunoreactive immunocyte-like cells in the *lamina propria* was higher in CIPO patients (**D**-vi) vs. controls or IBS cases.

(**E**) Histogram showing the significant decrease in the number of neurons per ganglion in the myenteric plexus observed in CIPO, compared to control tissue biopsies.

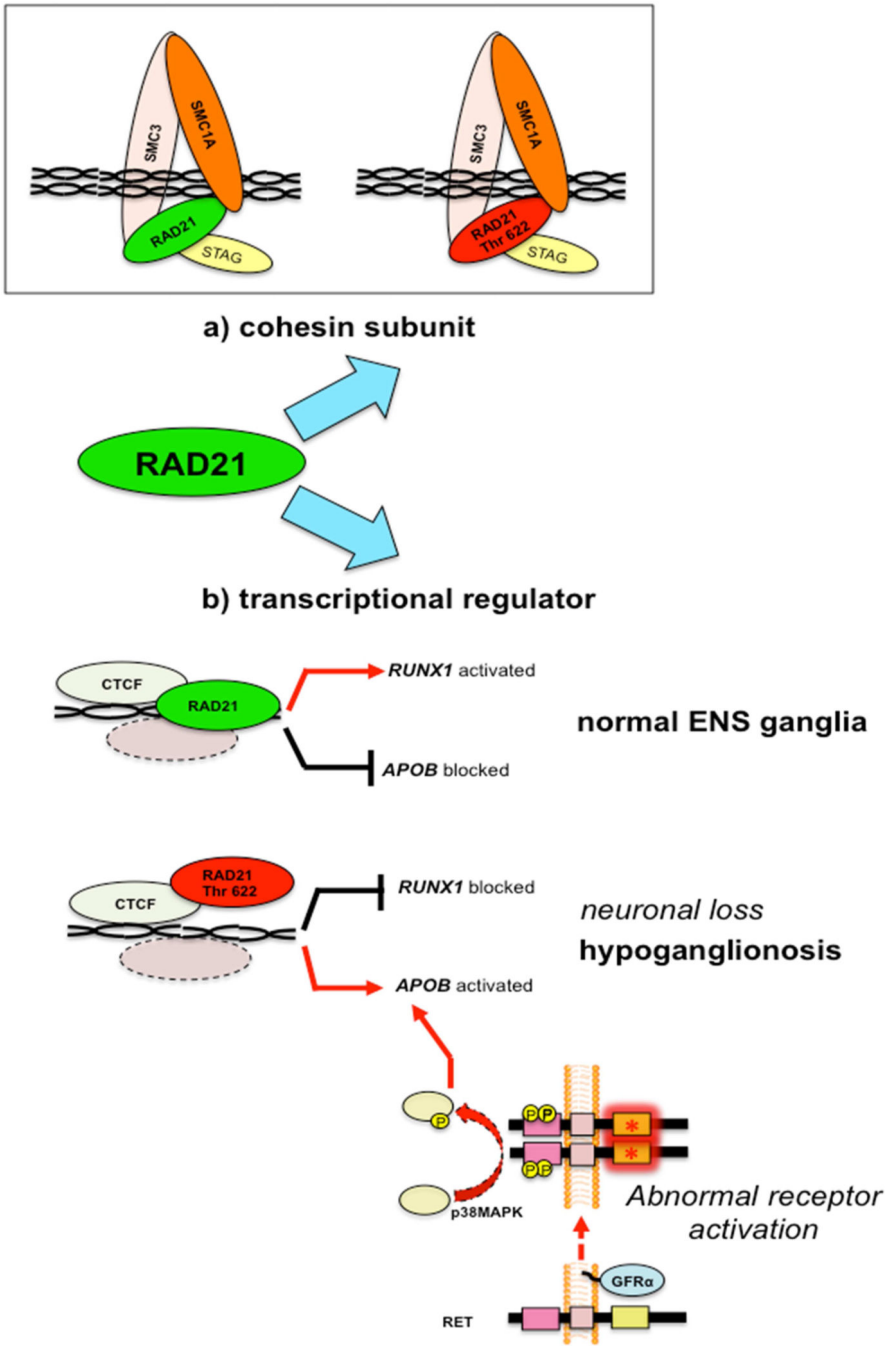

Figure 6. Model of RAD21 functioning as cohesin complex (A) or as transcription factor (B)

(A) RAD21 belongs to the cohesin complex regulating chromosomal replication. RAD21 p. 622Thr does not alter SMC1A subunit-binding. (**B**) Wild-type RAD21 promotes *RUNX1* and represses *APOB* expression. RAD21 p.622Thr downregulates *RUNX1* expression, de-represses APOB expression and leads to ENS neuron loss with resultant hypoganglionosis. Alternative pathways, including RET abnormal activation (e.g. the p.620 Cys>Arg mutation

[red asterisk] in heterozygous mice) can lead to APOB overexpression, which is phenotypically associated with hypoganglionosis.

Table 1

Clinical characteristics of idiopathic CIPO patients included in the *RAD21* mutation screening.

Patient reference code	Age	Sex	Feeding	Intestinal Manometry	Histopathology
SWE CIPO004	60	F	Oral	Severe hypomotility	Inflammatory neuropathy; severe depletion of ICC
SWE CIPO010	44	F	Oral+PPN	BUPA and absence of feeding activity	Inflammatory neuropathy
SWE CIPO035	60	F	Oral+PPN	Abnormally propagated AFs	Inclusion neuropathy
SWE CIPO042	56	F	TPN	---	Inflammatory neuropathy
SWE CIPO094	61	F	Oral	Abnormally configurated and propagated AFs; BUPA	Inclusion neuropathy
SWE CIPO095	49	F	Oral	BUPA	Inflammatory neuropathy
SWE CIPO096	56	F	Oral	BUPA; SPUPA; abnormally configurated and propagated AFs	Degenerative neuropathy; vacuolar myopathy
SWE CIPO097	41	F	EN+PPN	BUPA; absence of feeding activity	Inflammatory neuropathy
SWE CIPO099	50	F	Oral+PPN	BUPA; SPUPA	Degenerative neuropathy
SWE CIPO149	37	M	TPN	Bowel dilatation	Inflammatory neuropathy
SWE CIPO245	41	F	Oral+PPN	Bowel dilatation	Degenerative myopathy; atrophic desmosis
SWE CIPO247	20	F	TPN	Bowel dilatation	Degenerative myopathy
ITA CIPO08	17	M	EN	Bowel dilatation	Degenerative myopathy
ITA CIPO27	39	F	Modified oral	Abnormally configurated and propagated AFs; BUPA	Intrinsic neuropathy
ITA CIPO15	38	F	Modified oral	Abnormally propagated AFs	Intrinsic neuropathy
ITA CIPO18	40	F	Modified oral	---	Extrinsic neuropathy
ITA CIPO22	26	M	EN/oral	Abnormally configurated and propagated AFs; BUPA	Intrinsic neuropathy
ITA CIPO10	56	M	EN	---	---

Patient reference code	Age	Sex	Feeding	Intestinal Manometry	Histopathology
ITA CIPO37	21	F	EN/liquid diet/ integrators	Abnormally configurated and propagated AFs	Intrinsic neuropathy
ITA CIPO23	22	M	EN/oral	Abnormally configurated and propagated AFs; BUPA	Intrinsic neuropathy
ITA CIPO38	44	F	Oral	Abnormally configurated and propagated AFs	Severe depletion of ICC
ITA CIPO13	25	F	Oral	BUPA; clustered contractions during fasting	---
ITA CIPO36	18	F	Oral	---	Degenerative myopathy
ITA CIPO29	1	M	Oral	---	Extrinsic neuropathy
ITA CIPO39	16	F	EN/oral	---	---
ITA CIPO26	18	F	Oral	Abnormally configurated and propagated AFs; numerous BUPA	Intrinsic neuropathy
ITA CIPO25	40	M	EN/oral	Abnormally configurated and propagated AFs; numerous BUPA	Inflammatory neuropathy
ITA CIPO24	35	F	EN/oral	Abnormally configurated and propagated AFs; numerous BUPA	Degenerative myopathy
ITA CIPO16	67	F	EN/oral	---	---
ITA CIPO14	40	F	EN	Irregularly propagated clustered contractions	Degenerative myopathy
ITA CIPO33	20	M	EN/oral	Abnormally configurated and propagated AFs;	---
ITA CIPO17	54	F	EN	Lack of AFs; postprandial clustered contractions; BUPA;, propagated clustered contractions	Intrinsic neuropathy
ITA CIPO30	46	F	Modified oral	---	Extrinsic neuropathy

Abbreviations: AF, activity front(s); BUPA, bursts of uncoordinated phasic activity; EN, enteral nutrition; ICC, interstitial cells of Cajal; PPN, partial parenteral nutrition; TPN, total parenteral nutrition; SPUPA, sustained periods of uncoordinated phasic activity.